

A possible mechanism of ultrafast amorphization in phase-change memory alloys: an ion slingshot from the crystalline to amorphous position

This article has been downloaded from IOPscience. Please scroll down to see the full text article.

2007 J. Phys.: Condens. Matter 19 455209

(<http://iopscience.iop.org/0953-8984/19/45/455209>)

View [the table of contents for this issue](#), or go to the [journal homepage](#) for more

Download details:

IP Address: 129.252.86.83

The article was downloaded on 29/05/2010 at 06:31

Please note that [terms and conditions apply](#).

A possible mechanism of ultrafast amorphization in phase-change memory alloys: an ion slingshot from the crystalline to amorphous position

A V Kolobov^{1,2}, A S Mishchenko^{3,4}, P Fons¹, S M Yakubonya⁴ and J Tominaga¹

¹ Center for Applied Near-Field Optics Research (CanFor), National Institute of Advanced Industrial Science and Technology, 1-1-1, Higashi, Tsukuba 305-8562, Japan

² Institut Charles Gerhardt, UMR 5253 CNRS-UM2-ENSCM-UM1, PMDP, Université Montpellier II, Place Eugène Bataillon, Montpellier Cedex 5, France

³ CREST, Japan Science and Technology Agency (JST), AIST, 1-1-1, Higashi, Tsukuba 305-8562, Japan

⁴ RRC 'Kurchatov Institute', 123182, Moscow, Russia

E-mail: a.kolobov@aist.go.jp

Received 11 September 2007

Published 24 October 2007

Online at stacks.iop.org/JPhysCM/19/455209

Abstract

We propose that the driving force of the ultrafast crystalline-to-amorphous transition in phase-change memory alloys is caused by strained bonds existing in the (metastable) crystalline phase. For the prototypical example of $\text{Ge}_2\text{Sb}_2\text{Te}_5$, we demonstrate that upon breaking of the longer Ge–Te bond by photoexcitation, a Ge ion is shot from an octahedral crystalline to a tetrahedral amorphous position by the uncompensated force of strained short bonds. Subsequent lattice relaxation stabilizes the tetrahedral surroundings of the Ge atoms and ensures the long-term stability of the optically induced phase.

1. Introduction

Photo-induced phase transitions have attracted ongoing attention because of their application in storage devices [1, 2]. The properties required for commercial memory media, such as fast switching, stability of the photo-converted state, and high level cyclability, singled out the phase-change effect in Te-based chalcogenides. Commercially utilized materials are Ge–Sb–Te alloys, mainly in the form of $\text{Ge}_2\text{Sb}_2\text{Te}_5$ (GST) used in digital versatile discs (DVDs) DVD-RAM and Ag–In–Sb–Te (AIST) alloys used in DVD-RW [3]. $\text{Ge}_2\text{Sb}_2\text{Te}_5$ stands over a million cycles, the switching time is on the nanosecond timescale and even femtosecond pulses are sufficient to render the material amorphous [3].

As is typical for many optically sensitive materials [1, 2, 4], amorphous chalcogenides are intrinsically metastable and undergo various structural transformations under the influence of an

external perturbation, in particular light. What makes these materials special? It is very difficult to believe that a material will stand millions of melting/solidification cycles without degradation of parameters and an essentially specific mechanism should be found. The fundamentals of the phase-change mechanism are just starting to emerge but striking features of both groups of materials are: (i) the existence of longer and shorter bonds between similar pairs of atom types in the crystalline state [5, 6], (ii) bond shortening in the amorphous state [5–7], and (iii) a considerable degree of intrinsic disorder, manifested in high concentrations of vacancies in GST [8] and a random occupancy of sites in AIST [5]. The first feature suggests that certain bonds in the system are weaker and can be selectively broken, the second one is an indication of the local atomic structure in the two states being significantly different, and the last property points to a considerable concentration of defect levels in the gap.

In this paper, we propose a model that explains the unusual features of the structural changes in the class of phase-transition chalcogenides. We concentrate on changes in a typical compound, $\text{Ge}_2\text{Sb}_2\text{Te}_5$, although our generic statements, based on the similarity of properties (i)–(iii), are general for all phase-change compounds.

2. The structure of $\text{Ge}_2\text{Sb}_2\text{Te}_5$

In the metastable form of GST, Te ions form a well ordered face-centred cubic (fcc) sublattice, with Ge and Sb being displaced from the centre of the cell [6, 9, 10]. As a result, there are subsystems of shorter and longer bonds. The shorter Ge(Sb)–Te bond lengths are 2.83 Å and 2.91 Å, respectively. The longer bonds are in the order of ~ 3.15 Å. In addition, there are 20% vacancies on the Ge/Sb sites that are intrinsic to the structure [6] but the role and exact location of which is not definitely known⁵. It should be stressed that while the details of the intermediate- and long-range order of the crystal structure are still not completely clear, the best description to-date of the structure is a distorted rock-salt like structure with a large isotropic thermal displacement parameter.

2.1. Photoexcitation

It has been shown [6] that upon exposure to intense laser pulses Ge atoms switch from an octahedral position at the centre of the rock-salt cell into a tetrahedral position within the Te fcc sublattice (figures 1(a) and (b)) which is responsible for the fast performance and high stability of the medium. It was suggested [6] and subsequently unequivocally demonstrated by *ab initio* simulations [10] that the total energies of Ge–Sb–Te for these two structures are rather close, which explains why both states possess high stability. However, a very important question remains unanswered, namely, what drives the Ge atom to switch to a tetrahedral symmetry position upon photoexcitation?

It should be noted that even the shorter bonds in GST (2.83 Å for Ge–Te and 2.91 Å for Sb–Te) are significantly longer than the sum of the corresponding covalent radii ($r_{\text{Ge}} = 1.22$ Å, $r_{\text{Sb}} = 1.38$ Å, $r_{\text{Te}} = 1.35$ Å [11]), i.e. all bonds—assuming they are covalent—are stretched. This is a crucial assumption that has to be justified. To address this issue, we have measured bulk XPS spectra of $\text{Ge}_2\text{Sb}_2\text{Te}_5$ using high-energy synchrotron radiation as the excitation source. Our measurements yielded the following values for the bonding energies: Ge 3d—30.8 eV, Sb 3d_{5/2}—529.6 eV, Te 3d_{5/2}—573.2 eV. These values are similar to those in covalently bonded solids [12]. The absence of charge transfer has been independently deduced from *ab initio* simulations [10, 13].

⁵ After this work had been prepared we became aware of a relevant publication by Wuttig M *et al* 2007 *Nat. Mater.* **6** 122.

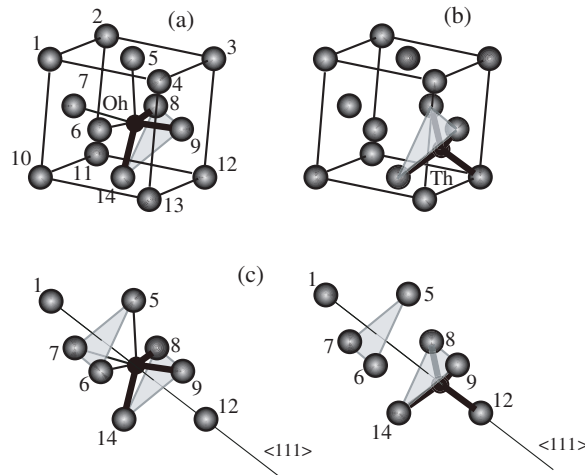


Figure 1. Fragments of the GST structures with the Te fcc lattice and a Ge atom located in the octahedral (a) and tetrahedral (b) symmetry sites. Other Ge (and Sb) atoms are not shown. The lower panel (c) shows the molecular fragments (8 Te atoms and 1 Ge atom) within which the Ge switching is considered.

It would seem that a simple decrease in the lattice parameter would have reduced the strains, thus lowering the total energy. However, the system prefers a larger lattice parameter and stretched (strained) bonds. The most plausible explanation for this is the fact that the Te fcc sublattice is intrinsically much stronger than the Ge(Sb)–Te interaction [6]. In line with this is also the fact that Si–Te bond lengths for octahedrally and tetrahedrally coordinated Si in Si_2Te_3 have the same lengths [14] as those for Ge–Te, although Si has a covalent radius that is significantly (0.11 Å) smaller than that of Ge.

2.2. A simple energy calculation

As already stated above, the details of the structure beyond the short-range order (i.e. including just a few atoms) are not known in either crystalline or amorphous cases. For this reason any reliable modern solid-state calculations are not possible: one is naturally limited to a very crude short-range order model. To the first approximation we can consider that Ge ions switch within a rigid Te sublattice as shown in figures 1(a) and (b). As the simplest model we can consider motion of a relatively light Ge ion within the eight nearest (and heavy) Te atoms (figure 1(c)).

Based on very simple considerations the potential experienced by the Ge ion located at distance d from a Te ion can be expressed in terms of a standard ion–ion interaction relation:

$$E(d) = C/d^4 \pm 2\sqrt{V_2^2 + V_3^2}, \quad (1)$$

where $V_2 = A/d^2$ is the covalent energy, V_3 is the independent of distance polar energy, and the first term is the interionic repulsion [15, 16]. In equation (1) the plus and minus signs correspond to bonding and antibonding states, respectively.

To determine the parameters of the interaction we used covalent radii $r_{\text{Ge}} = 1.22$ Å and $r_{\text{Te}} = 1.35$ Å to get the equilibrium of potential at $d_0 = 2.57$ Å which, implying the condition $\partial E(d)/\partial d = 0$, fixes the repulsion parameter $C = A^2/\sqrt{V_3^2 + A^2/d_0^4}$. The polar energy $V_3 = 1.66$ eV is determined in [16] and a reasonable value of covalent attraction $V_2 = 2$ eV [16] in equilibrium gives $A = 13.2$ eV Å². With the above parameters we have calculated the

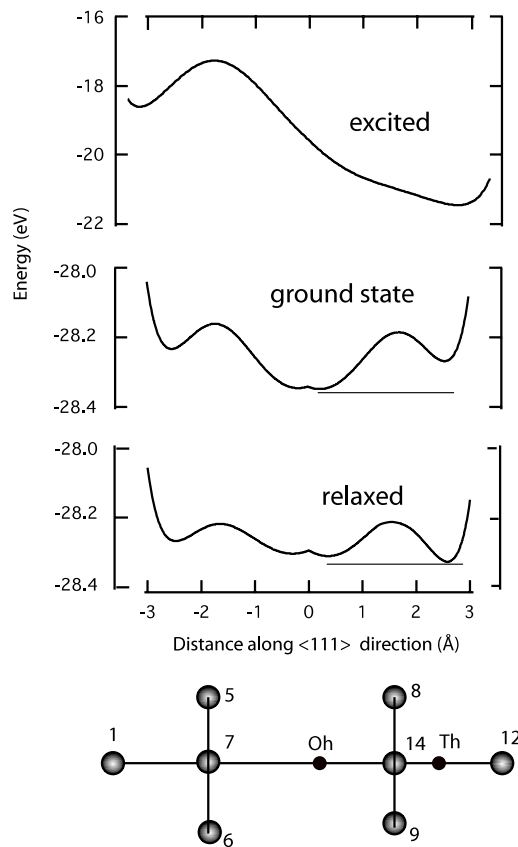


Figure 2. Potentials for the Ge atom in the field of eight Te atoms in the ground state and in the state where one of the weak bonds is excited (upper panel)⁶. The schematic drawing represents the considered molecule. The lower panel demonstrates the stabilization of the tetrahedral geometry by relaxation of the network after Te atoms 5, 6, 7 have been moved away in the direction perpendicular to the axis by 0.1 Å.

potential for a Ge atom moving within a rigid Te lattice along the [111] direction as shown in figure 1(c).

The ‘ground-state’ curve in figure 2 presents the potential in the ground state. The origin of the coordinate r —which represents the position of the Ge atom along the 111 axis—corresponds to the centrosymmetric position of Ge between the two Te triangles shown in figure 1(c). The experimental positions of Ge are $r_{\text{cr}} = 0.33$ Å in the crystalline state and $r_{\text{am}} = 2.6$ Å in the amorphous state.

It is seen that the very simple form of interaction (1) reproduces general features of the system with the crystalline global minimum at $r \approx 0$ and higher amorphous local minima at $r \approx 2.6$ Å. In addition, although the minima of potential (1) from three Te ions (located off the [111] axis) to the right (left) correspond to $r = 0.86$ Å ($r = -0.86$ Å), the joint action of left and right Te ions creates a broad minimum at $r \approx 0$.

⁶ Since we have used a very simple cell consisting of just nine atoms (one germanium and eight tellurium atoms) the obtained energies have typically molecular values. As we have used the ground-state parameters, the absolute energy values obtained for the excited state are likely to be different. In a solid, the energy levels will split into bands but this must not effect the main characteristics, in particular, the force acting on an excited Ge atom is much larger than the characteristic energies of the ground-state potential.

From the Jahn–Teller theorem it is known [17, 18] that centrosymmetric structures are locally unstable and centrosymmetric positions in solids are allowed as a consequence of long-range stabilizing forces that occur within a macroscopic periodic lattice. For the case of GST, the high concentration (20%) of vacancies destroys the long-range order, leading to the formation of the non-centrosymmetric distorted rock-salt structure. This is evidenced by the loss of long-range order in the Ge/Sb sublattice, as opposed to the well defined Te sublattice where longer-range spatial correlations are clearly visible [6].

To reproduce the displacement of the Ge atom from the centrosymmetric position we introduce a Jahn–Teller coupling λ and a coupling to an external electric field ξ caused by non-symmetric distribution of vacancies in the Ge/Sb sublattice. The above interactions create an additional potential [17]

$$\Delta E(r) = -\sqrt{\mathcal{N}^2 + \lambda^2 r^2} - \xi r. \quad (2)$$

We chose the values $\lambda = 0.08 \text{ eV \AA}^{-1}$ and $\xi = 0.007 \text{ eV \AA}^{-1}$ to reproduce the experimental position of Ge. The non-adiabatic matrix element $\mathcal{N} = 0.0006 \text{ eV}$ does not change the potential significantly though makes it possible to avoid an unphysical jump of the second derivative of potential at $r = 0$.

When an electron on one of the (long) bonds is transferred to the antibonding orbital due to photoexcitation⁷, the potential changes drastically (figure 2, the ‘excited’ curve). In particular, in the excited state there appears a force acting on the Ge ion. The excited Ge ion relaxes into a position corresponding to the minimum located at 2.6 \AA , i.e. at the tetrahedral position. We estimated the relaxation time to be on the scale of 10^{-13} s (the inverse of the phonon frequency) and the atom travels a distance of about 2 \AA . A simple estimate gives an impressive speed of $\approx 10^3 \text{ m s}^{-1}$. A simple analogy of the process is a slingshot shooting a Ge atom.

At the same time, the (5, 6, 7) Te atoms that were previously bonded to the Ge atom by the longer bonds experience a stronger interaction with the Sb atoms located on the other side (Sb atoms are not shown in the figure). The Sb–Te bonds shrink by about 0.1 \AA as evidenced by the EXAFS data [6], resulting in a Te lattice distortion (see figure 5 of [22]). If the three (5, 6, 7) Te atoms move away from the axis by 0.1 \AA , the tetrahedral geometry becomes the lowest in energy, as shown in the lower panel of figure 2 (‘relaxed’ curve). The lattice relaxation thus stabilizes the tetrahedral position of the Ge atom. The energy barrier, separating the octahedral and tetrahedral sites is of the order of $0.1\text{--}0.2 \text{ eV}$ in our simple model, which is similar to the value obtained through advanced *ab initio* simulations [23].

2.3. Laser excitation

An important issue is why one needs intense laser pulses to induce the phase change. Vacancies in semiconductors are known to produce deep donor states [25, 24]. The presence of a very large concentration of vacancies in the $\text{Ge}_2\text{Sb}_2\text{Te}_5$ structure thus leads to the chemical potential being pinned near the valence band. The local switching of Ge from octahedral to tetrahedral coordination in the dilute limit gives rise to complex defects (a vacancy plus an interstitial Ge atom) within the rock-salt structure with corresponding states in the gap. Since the total energies of $\text{Ge}_2\text{Sb}_2\text{Te}_5$ containing Ge atoms in octahedral and tetrahedral symmetry positions are very close [10], we can expect energy levels corresponding to individual tetrahedrally coordinated Ge atoms (and corresponding vacancies) to be located closer to the valence band.

⁷ Photo-induced rupture of *weaker* bonds in chalcogenides has been demonstrated to be responsible for a thermal photo-induced melting of amorphous Se [19]. Photoexcitation was also found to play a major role in photo-crystallization of Se [20] and photo-induced amorphization of AsSe [21]. Since the top of the $\text{Ge}_2\text{Sb}_2\text{Te}_5$ valence band is predominantly formed by the states due to Te and Ge atoms [13] we consider the excitation of the weaker Ge–Te bonds.

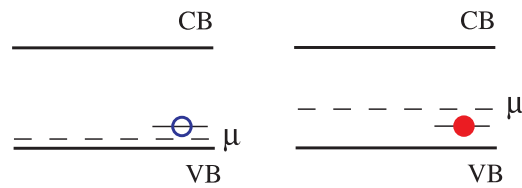


Figure 3. Schematic energy band structure of $\text{Ge}_2\text{Sb}_2\text{Te}_5$ at low (left) and high (right) excitation levels.

(This figure is in colour only in the electronic version)

At room temperature and at low-excitation levels, the states of the complex defects are located above the chemical potential and are hence unoccupied, as seen in figure 3, left. In this situation, a single excitation event results in an unstable tetrahedral Ge site which readily decays back to the original structure. Under intense optical excitation, the chemical potential moves towards mid-gap. In this situation the defect states are located below the chemical potential and are now occupied (stable) (figure 3, right). Once the concentration of these defects becomes sufficiently large and their wavefunctions overlap, the electronic structure changes to that of the ‘amorphous’ state.

The same result can—in principle—be achieved by heating. Indeed, our recent XANES measurements (not shown here) have demonstrated that, upon melting, Ge atoms acquire tetrahedral symmetry positions. There is, however, a very important difference. A focused laser beam excites a very small volume and upon cessation of the laser pulse the heat can dissipate fast enough to leave the newly created structure stable. With thermal heating, the heated volume is large and cannot be quenched fast enough; the system can overcome the energy barrier between the amorphous and crystalline states, eventually producing the crystalline phase.

We would like to stress here that the transition into the tetrahedral structure is localized, i.e. upon rupture of the longer Ge–Te bonds *individual* Ge atoms switch due to a force acting on them in the excited state. This process is extremely fast. To restore the original structure, on the other hand, long-range interactions are important. This process requires motion of *many* atoms and for this reason crystallization is a slower process than amorphization. It is possible that collectiveness of the crystallization process is the reason why the experimentally measured activation energy for the crystallization is higher than the energy barrier for an individual transition.

3. Conclusion

To conclude, we suggest that photoexcitation of a weak Ge–Te bond in a distorted rock-salt structure produces a net force acting on the Ge ions along the [111] direction which drives the phase transition towards the so-called amorphous state. The subsequent distortion of the Te lattice stabilizes the tetrahedral structure which ensures the stability of the recorded bit. Whilst the detailed discussion above refers to a specific material, the similarity is crucial for our mechanism properties (i)–(iii) in all phase-transition chalcogenides and is indicative of a similar transformation mechanism in all of them. Namely, the transition is initiated by photoexcitation of the weaker bonds and subsequent lattice relaxation stabilizes the newly established local structure. A necessity for the shift of the chemical potential towards mid-gap that is needed to stabilize the tetrahedral sites is the reason why this process requires high photon fluxes.

While for the most part we concentrated on photoexcitation of the weak bonds, we believe that the above considerations are also valid for electronic memory devices when the material is switched between the two states by intense current pulses. Application of high electric fields

leads to the injection of charge carriers from the electrodes that are likely to behave in a similar way to photoexcited carriers.

Acknowledgment

ASM acknowledges support of the Russian Foundation for Basic Research grant 07-0200067-a.

References

- [1] Nasu K (ed) 1997 *Relaxation of Excited States and Photoinduced Structural Phase Transitions* (Berlin: Springer)
- [2] Kolobov A V (ed) 2003 *Photo-Induced Metastability in Amorphous Semiconductors* (Weinheim: Wiley–VCH)
- [3] Ohta T and Ovshinsky S R 2003 *Photo-Induced Metastability in Amorphous Semiconductors* ed A V Kolobov (Weinheim: Wiley–VCH) p 310
- [4] Koshihara S, Tokura Y, Takeda K and Koda T 1992 *Phys. Rev. Lett.* **68** 1148
- [5] Matsunaga T, Umetani Y and Yamada N 2001 *Phys. Rev. B* **64** 184116
- [6] Kolobov A V, Fons P, Frenkel A I, Ankudinov A L, Tominaga J and Uruga T 2004 *Nat. Mater.* **3** 703
- [7] Tani K, Yiwata N, Harigaya M, Emura M and Nakata Y 2001 *J. Synchrotron Radiat.* **8** 749
- [8] Yamada N and Matsunaga T 2002 *J. Appl. Phys.* **88** 7020
- [9] Shamoto S, Yamada N, Matsunaga T, Proffen Th, Richardson J W Jr, Chung J H and Egami T 2005 *Appl. Phys. Lett.* **86** 081904
- [10] Welnic W, Pamungkas A, Detemple R, Steimer C, Blugel S and Wuttig M 2006 *Nat. Mater.* **5** 56
- [11] <http://www.webelements.com>
- [12] *Handbook of X-ray Photoemission Spectroscopy* 1995 Physical Electronics Inc.
- [13] Robertson J, Xiong K and Peacock P W 2007 *E-MRS Spring Mtg 2006 (Nice)* at press
- [14] Petersen K E, Birkholz U and Adler D 1973 *Phys. Rev. B* **8** 1453
- [15] Harrison W A 1980 *Electronic Structure and the Properties of Solids* (San Francisco, CA: Freeman)
- [16] Harrison W A and Ciraci S 1974 *Phys. Rev. B* **10** 1516
- [17] Bersuker I B 1983 *The Jahn–Teller Effect* (New York:IFI/Plenum)
- [18] Kristoffel N and Zavt G 1968 *Localized Excitations in Solids* ed R F Wallis (New York: Plenum) p 132
- [19] Poborchii V, Kolobov A V and Tanaka K 1999 *Appl. Phys. Lett.* **74** 215
- [20] Roy A, Kolobov A V and Tanaka K 1998 *J. Appl. Phys.* **83** 4951
- [21] Elliott S R and Kolobov A V 1991 *J. Non-Cryst. Solids* **128** 216
- [22] Kolobov A V, Fons P, Tominaga J, Frenkel A I, Ankudinov A L, Yannopoulos S N, Andrikopoulos K S and Uruga T 2005 *Japan. J. Appl. Phys.* **44** 3345
- [23] Robertson J, Xiong Ka and Peacock P 2006 *Mater. Res. Soc. Symp. Proc.* **918** H01–02
- [24] Baraff G A, Kane E O and Schlüter M 1980 *Phys. Rev. B* **21** 5662
- [25] Newton J L, Chatterjee A P, Harris R D and Watkins G D 1983 *Physica B* **116** 219